2021 43rd Annual International Conference of the
IEEE Engineering in Medicine & Biology Society (EMBC)
Oct 31 - Nov 4, 2021. Virtual Conference

3D Reconstruction of Carotid Artery from Ultrasound Images

Yingnan Ma, Zining Wang, Xu Dai, Bofeng Chen, Anup Basu
Department of Computing Science, University of Alberta

***Abstract*— 3D reconstruction is an important area in computer vision, which can be applied to assist in medical diagnosis. Compared to observing 2D ultrasound images, 3D models are more suitable for diagnostic interpretation. In this paper, we describe an approach for 3D reconstruction of the carotid artery utilizing ultrasound images from the transverse and longitudinal views. We implement a human-computer interface to ensure the accuracy of the segmentation results by involving superpixels and ellipse fitting techniques. This approach is expected to achieve better accuracy to assist diagnostics in the future.**

I. Introduction

Ultrasound diagnostic technology is widely utilized for early clinical detection due to its innocuity. When ultrasound waves come into the human body, it is reflected, refracted, and absorbed by the human tissues. Doctors can distinguish diseases by interpreting the features of ultrasound images. 3D reconstruction is pursued to improve the accuracy of a diagnosis. Differing from observing ultrasound images, 3D models can allow doctors to check details from different point of views, which can help in making more informed decisions. To achieve 3D reconstruction, the tasks can be separated into two categories: image segmentation and 3D modeling.

In the state-of-the-art, many segmentation methods have been proposed. Otsu's method [1] is a thresholding based segmentation algorithm that divides grayscale images into foreground and background by selecting a threshold. Otsu's method can automatically select the appropriate threshold [2] according to the variance of the foreground and background. The value of the inter-class variance [3] is proportional to the difference between the foreground and background. To optimize the segmentation results, filtering methods are deployed to weaken the influence of noise in an image. Kalman filtering [4] is a popular approach for reducing the effect of noise. It is widely used for tracking and positioning blood vessels [5] [6] in real time. In addition to Otsu's method, the Active Contour model [7] can also achieve image segmentation. It utilizes curve evolution to detect the target in a given image based on edge information. By minimizing the energy function [8], the curve changes are initiated to approach the target edge. The active models are improved in [9] by introducing the ability to converge in concave regions of a contour. After the segmentation, modeling methods are applied for 3D reconstruction. To project 2D images into 3D, images from different point of views [10] are necessary. In the state-of-the-art, 3D models are usually represented in three ways: polygonal meshes, voxels (volumetric pixel) and point clouds. Compared to voxels, point clouds can express a 3D model with smaller grids, which does not result in significant loss of detail. Compared to point clouds, polygonal meshes need much less storage to display surface information with similar visual detail.

To design a precise and efficient 3D reconstruction method for a carotid artery, we implement a human-computer interface to ensure the accuracy of the segmentation results. We utilize superpixel and ellipse fitting techniques to optimize the segmentation results so that the accuracy of the model can be ensured. To demonstrate the modeling performance, we generate results using both point clouds and polygonal meshes.

II. Methodology

In this section, we separate the proposed approach into four subsections. The first subsection introduces the image pre-processing steps. The second subsection introduces the segmentation approach. The third subsection introduces the optimization step by utilizing superpixel and ellipse fitting. The final subsection introduces the modeling step. The pipeline of the proposed method can be seen in Fig.1.

A. Image pre-processing

Considering the poor quality of ultrasound images, we first implement image pre-processing methods. This way, we can avoid noise impacting segmentation results. For image pre-processing, we involve median filter, histogram equalization, Gaussian filter, dilation, and erosion techniques. In ultrasound images, we can clearly notice different types of noise, such as Gaussian noise and salt and pepper noise, which can significantly reduce image quality. To remove the mixed noise, we apply a double-filtering algorithm to remove the noise before and after histogram equalization. We first implement the median filter [11] to coarsely reduce noise. After this noise removal, the Gaussian noise can been effectively controlled. Noise reduction can help the target object stand out in ultrasound images. As shown in Fig.1, Gaussian noise is removed from the ultrasound image; but, the salt and pepper noise can still be observed.

To further improve image quality, we apply histogram equalization [12] to make the details of the ultrasound image clearer so that the remaining noise can be easily identified. After the histogram is normalized, the outline of the carotid artery cross-section becomes easier to recognize. From Fig.1 we can see that the salt and pepper noise has become more obvious. To remove the noise shown in the histogram equalization results, we apply a Gaussian filter [13]. Gaussian

978-1-7281-1178-0/21/$31.00 ©2021 IEEE

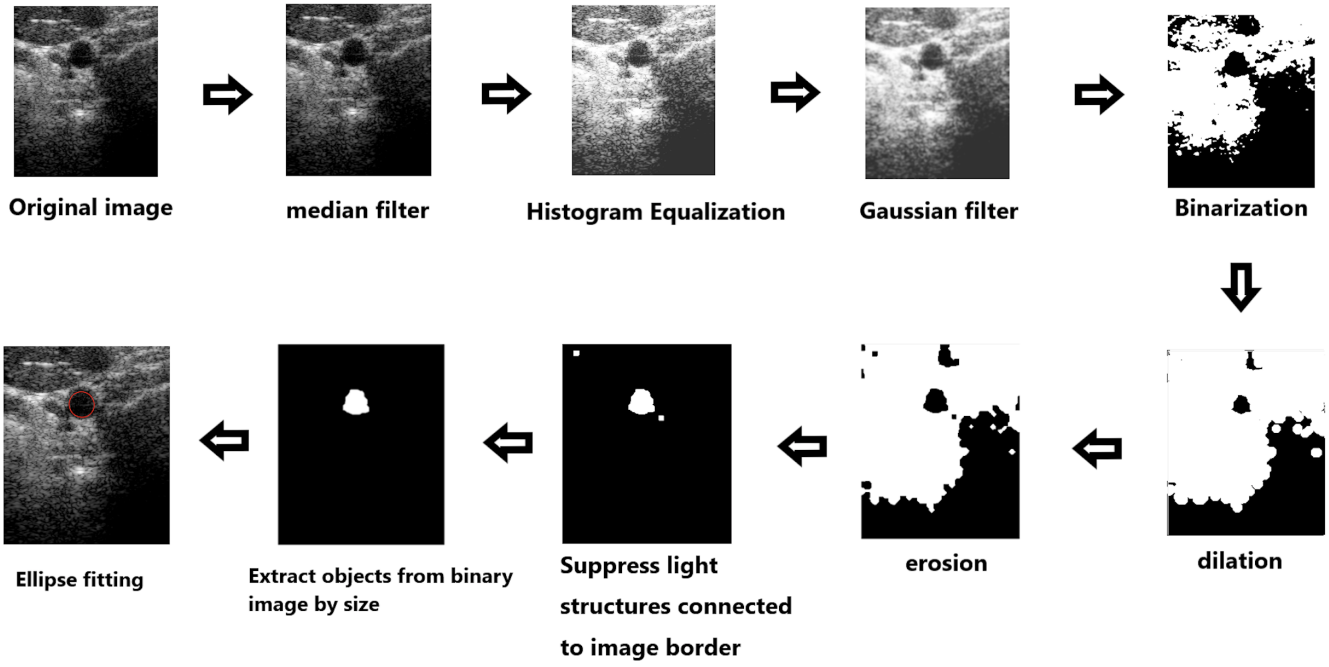

Fig. 1. Pipeline of the proposed method.

blur can smooth an image and highlight the target object. A two-dimensional Gaussian function is represented as:

$$h(x,y) = e^{-\frac{x^2+y^2}{2\sigma^2}} \tag{1}$$

In this equation, (x, y) represents point coordinates, which can be considered as integers in image processing; σ is the standard deviation. To obtain a Gaussian filter template, the Gaussian function can be discretized, and the resulting value of the Gaussian function used as the coefficient of the template. The size of the template is set to $(2k+1)(2k+1)$. The formula to compute the value of each element in the template is given by:

$$H_{i,j} = \frac{1}{2\pi\sigma^2} e^{-\frac{(i-k-1)^2+(j-k-1)^2}{2\sigma^2}} \tag{2}$$

After blurring, the salt and pepper noise appearing at the bottom of the image are partially removed. Also, the transverse and longitudinal sections of the carotid artery have a better separation from the background.

In addition to the above double-filtering algorithm, we also applied erosion and dilation to remove the salt and pepper noise in the binary image. Erosion and dilation can help retain the details of target objects and remove unnecessary noise. After erosion and dilation, the main body is further highlighted. Because we only need to keep the cross-section of the carotid artery for ellipse fitting, our final task is to extract objects from a binary image by size, and suppress unimportant structures connected to image borders.

B. Segmentation

After the pre-processing, we implement Otsu's method to achieve a coarse segmentation. Following Otsu's method, superpixel and ellipse fitting techniques are applied to optimize the segmentation result. Otsu's method obtains the segmentation threshold according to the equations below.

$$N0 + N1 = M * N \tag{3}$$

$$\mu = \omega 0 * \mu 0 + \omega 1 * \mu 1 \tag{4}$$

$$g = \omega 0 \omega 1 (\mu 0 - \mu 1)^2. \tag{5}$$

This is the traversal method to obtain the threshold that maximizes the between-class variance g, which is required for Otsu's method.

After implementing Otsu's method, we also apply the $bwboundaries$ function to obtain the contours of target objects in a binary graph, including external contours and internal edges. In a binary image, the object must be composed of non-zero pixels, with 0 representing the background. B is a P×1 cell array, where P represents the number of objects. Each cell is a Q×2 matrix corresponding to the coordinates of the contour pixels of the object, where Q represents the number of the contour pixels. Each row in the Q×2 matrix represents the position coordinates of the boundary pixels of the connected body. After applying the $bwboundaries$ function [14], we can find the connected domain of the image, which is the region we need to extract.

Based on the previous segmentation results, we use the superpixel technique to improve segmentation accuracy. The superpixel technique can group pixels into blocks based on the intensity information of neighbours. According to the number of foreground pixels appearing in each block, we

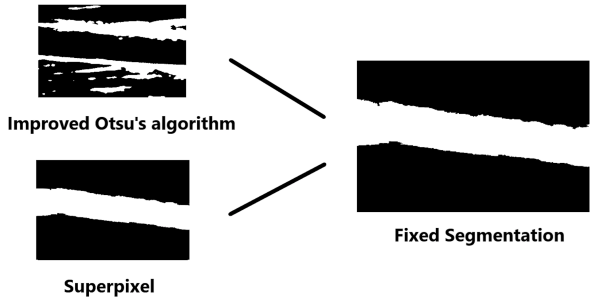

Fig. 2. Comparison of the fitting results of different segmentation methods.

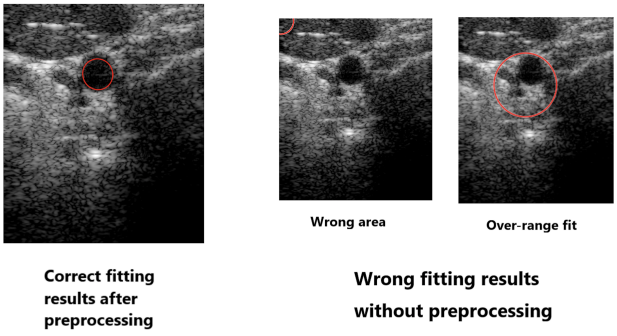

Fig. 3. Comparison of results of different segmentation methods.

can mark each superpixel block as foreground or background. This way, the coarse segmentation results can be optimized. In our segmentation process, superpixels are mainly used to segment the longitudinal section of the carotid artery. We also use the SLIC algorithm [15] for auxiliary segmentation. This algorithm can partition a picture by color. After partitioning, we use manual interaction to select the required area, and then extract the longitudinal section of the carotid artery. After extracting the longitudinal section of the carotid artery from the super-pixel image, the method compares the longitudinal section obtained by Otsu's method, and then correct the segmentation results.

C. Ellipse fitting

The cross section of the carotid artery is usually round. Traditional segmentation methods do not identify precise circles. Thus, we use an ellipse fitting method to fit the cross-sectional shape of the carotid artery to achieve a better segmentation effect. The fitting method uses the conic equation. The equation of an ellipse is:

$$x^2 + Axy + By^2 + Cx + Dy + E = 0 \tag{6}$$

This equation measures points on the ellipse contour. To find the best matching ellipse, we need to minimize F according to the principle of least squares. The equations for this are:

$$\frac{\partial \mathrm{F}}{\partial \mathrm{A}} = \frac{\partial \mathrm{F}}{\partial \mathrm{B}} = \frac{\partial \mathrm{F}}{\partial \mathrm{C}} = \frac{\partial \mathrm{F}}{\partial \mathrm{D}} = \frac{\partial \mathrm{F}}{\partial \mathrm{E}} = 0 \tag{7}$$

$$\mathbf{D} = \begin{pmatrix} x_1^2 & x_1 y_1 & y_1^2 & x_1 & y_1 & 1 \\ \vdots & \vdots & \vdots & \vdots & \vdots & \vdots \\ x_i^2 & x_i y_i & y_i^2 & x_i & y_i & 1 \\ \vdots & \vdots & \vdots & \vdots & \vdots & \vdots \\ x_N^2 & x_N y_N & y_N^2 & x_N & y_N & 1 \end{pmatrix} \tag{8}$$

To fit an ellipse the following five parameters need to be calculated: position parameters (θ, x_0, y_0) and shape parameters (a, b).

D. 3D modeling

After obtaining the fitted ellipse for the carotid artery, we can use the ellipse equation to perform polynomial fitting, and then generate a visual point cloud of the carotid artery. Since point clouds lack neighborhood and topology information, it is not easy to generate the surface directly. We use Delaunay-based methods [16] to convert the point cloud into a mesh. The 3D reconstruction methods are based on scattered point clouds [17]. The main idea of this method is to explore the possible neighbors of all sample points in all directions from scattered point data. Thus, we need to triangulate [16] the point cloud data, and then extract the triangles related to the geometric shape. To achieve this goal, we utilize the Crust algorithm [18] proposed by Amenta. Let S represent the set of sample points of a smooth curve in a two-dimensional space. Then, the Crust algorithm can compute the Voronoi diagram of S. Following this, we can get a set of poles represented by P. For each sample point s, if s is not in the convex hull of S, p^+ is the farthest point of the Voronoi diagram corresponding to S. If s is in the convex hull of S, then p^+ is designated as a point at infinity outside the convex hull. Consider the outer vector along sp^+ at s. If there is a point p in the Voronoi diagram of the point set S, which satisfies $\angle p^+ sp$ greater than π /2, and is farther from other vertices s, then p is regarded as another pole sp^+. By calculating the Delaunay triangulation of $S \bigcup P$ and keeping triangles for which all vertices are sample points, we can obtain a linear surface.

III. Experiments

A. OTSU Threshold

In general, Otsu's method traverses all pixels from intensity 0 to 255 for gray scale images. For a gray scale image with two peaks in the histogram, the value of T obtained by Otsu's method is approximately equal to the trough between the two peaks. The calculated threshold must be between the two peaks. By observing the image of the carotid artery, we find that the histograms of ultrasound images are single peaked, where the threshold T should be around the peak. To calculate the threshold, we only consider existing intensity range. As shown in Fig.4, we only take intensity range (0,230) into consideration when Otsu traverses the pixels. The intensity range with few pixels is ignored during the traversal. Thus, only the inter-class variance between the modified intensity range areas is calculated. This reduces some unnecessary calculations, and increases the computational efficiency by 37 percent.

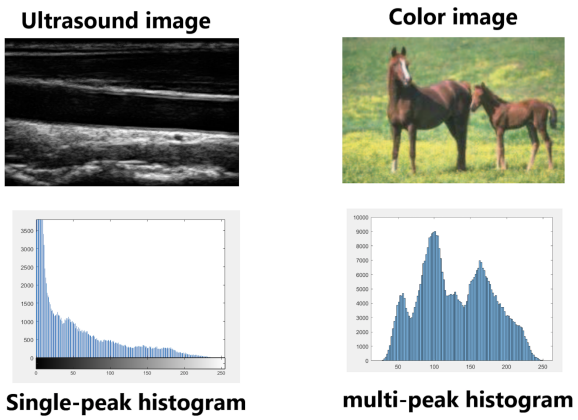

Fig. 4. The histogram of an ultrasound image is usually single-peaked, and a colored image is usually multi-peaked. Otsu's method can be simplified based on this observation to improve efficiency.

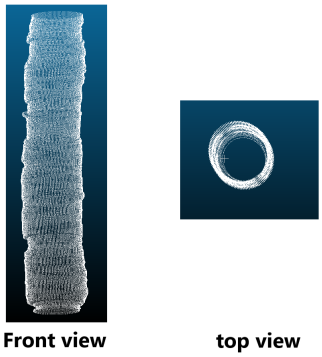

Fig. 5. Point clouds from various perspectives.

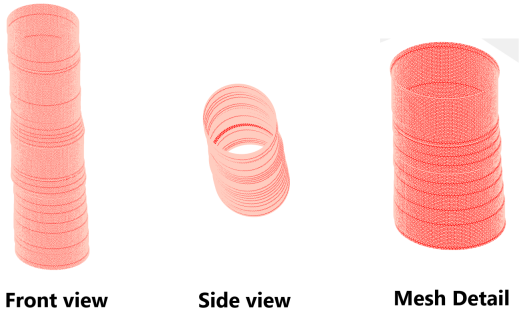

Fig. 6. Mesh from various perspectives.

B. Segmentation and Modeling Results

Ultrasound images contain unclear edges and mixed noise. Thus, the segmentation result of the traditional Otsu's method expands the segmentation range and makes the segmentation results inaccurate. Helped by the pre-processing strategy, the accuracy of ellipse fitting can be significantly improved. This improvement can be seen in Fig.3. By utilizing the superpixel method, the overall segmentation effect can be improved by selecting the longitudinal-section of the carotid artery in the superpixel area. The improvement achieved by superpixels can be seen in Fig.2. The superpixel method can effectively reduce the segmentation range of Otsu's method. The final 3D modeling results can be seen in Fig.5 and Fig.6, where Fig.5 represents the point cloud model and Fig.6 represents the mesh model.

IV. Conclusion

We proposed a high-precision 3D reconstruction method for the carotid artery. Utilizing ultrasound images of the cross section and the longitudinal section, we successfully built the point cloud and mesh models of the carotid artery. We applied a double filtering strategy to achieve noise removal from ultrasound images. Following Otsu's method, we creatively utilized superpixel and ellipse fitting techniques to optimize the segmentation results. The proposed approach is expected to have better accuracy and assist in diagnostics in the future.

References

[1] N. Otsu, "A threshold selection method from gray-level histograms," *IEEE transactions on systems, man, and cybernetics*, vol. 9, no. 1, pp. 62–66, 1979.

[2] D. Liu and J. Yu, "Otsu method and k-means," in *2009 Ninth International Conference on Hybrid Intelligent Systems*, vol. 1. IEEE, 2009, pp. 344–349.

[3] W. A. Mustafa and H. Yazid, "Background correction using average filtering and gradient based thresholding," *Journal of Telecommunication, Electronic and Computer Engineering (JTEC)*, vol. 8, no. 5, pp. 81–88, 2016.

[4] R. Kalman, "A new approach to linear filtering and prediction problems" transaction of the asme journal of basic," 1960.

[5] H. Musoff and P. Zarchan, *Fundamentals of Kalman filtering: a practical approach*. American Institute of Aeronautics and Astronautics, 2009.

[6] J. Guerrero, S. E. Salcudean, J. A. McEwen, B. A. Masri, and S. Nicolaou, "Real-time vessel segmentation and tracking for ultrasound imaging applications," *IEEE Transactions on Medical Imaging*, vol. 26, no. 8, pp. 1079–1090, 2007.

[7] M. Kass, A. Witkin, and D. Terzopoulos, "Snakes: Active contour models," *INTERNATIONAL JOURNAL OF COMPUTER VISION*, vol. 1, no. 4, pp. 321–331, 1988.

[8] V. Caselles, "A geometric model for active contours in image processing," *Numerische Mathematik*, vol. 36, no. 2, pp. 256 – 273, 1993. [Online]. Available: http://10.1007/BF01385685

[9] T. Wang, I. Cheng, and A. Basu, "Fluid vector flow and applications in brain tumor segmentation," *IEEE transactions on biomedical engineering*, vol. 56, no. 3, pp. 781–789, 2009.

[10] C.-H. Lin, C. Kong, and S. Lucey, "Learning efficient point cloud generation for dense 3d object reconstruction," 2017.

[11] D. R. Brownrigg, "The weighted median filter," *Communications of the ACM*, vol. 27, no. 8, pp. 807–818, 1984.

[12] S. M. Pizer, E. P. Amburn, J. D. Austin, R. Cromartie, A. Geselowitz, T. Greer, B. ter Haar Romeny, J. B. Zimmerman, and K. Zuiderveld, "Adaptive histogram equalization and its variations," *Computer vision, graphics, and image processing*, vol. 39, no. 3, pp. 355–368, 1987.

[13] G. Deng and L. Cahill, "An adaptive gaussian filter for noise reduction and edge detection," in *1993 IEEE conference record nuclear science symposium and medical imaging conference*. IEEE, 1993, pp. 1615–1619.

[14] R. C. Gonzalez, S. L. Eddins, and R. E. Woods, *Digital image publishing using MATLAB*. Prentice Hall, 2004.

[15] R. Achanta, A. Shaji, K. Smith, A. Lucchi, P. Fua, and S. Süsstrunk, "Slic superpixels," Tech. Rep., 2010.

[16] T. Su, W. Wang, Z. Lv, W. Wu, and X. Li, "Rapid delaunay triangulation for randomly distributed point cloud data using adaptive hilbert curve," *Computers & Graphics*, vol. 54, pp. 65–74, 2016.

[17] L. Giaccari, "Surface reconstruction from scattered points cloud," Tech. Rep., 2010.

[18] Amenta, "Crust algorithm," Tech. Rep., 1997.